J. Phys. D: Appl. Phys. **42** (2009) 105409 (8pp) doi:10.1088/0022-3727/42/10/105409

Structural characterization of two-step growth of epitaxial ZnO films on sapphire substrates at low temperatures

P Pant[1,4], J D Budai[2], R Aggarwal[1], R J Narayan[1,3] and J Narayan[1]

[1] Department of Materials Science and Engineering, EB-I, Centennial Campus, North Carolina State University, Raleigh, NC 27695-7907, USA
[2] Materials Science and Technology Division, Oak Ridge National Laboratory, Oak Ridge, TN 37831-6030, USA
[3] Joint Department of Biomedical Engineering, University of North Carolina, Chapel Hill, NC 27599, USA

E-mail: ppant@ncsu.edu

Received 6 December 2008, in final form 26 March 2009
Published 29 April 2009
Online at stacks.iop.org/JPhysD/42/105409

Abstract
We have investigated two-step growth of high-quality epitaxial ZnO films, where the first layer—the buffer layer (nucleation layer template)—is grown at a low temperature (230–290 °C) to induce a smooth (two-dimensional) growth. This is followed by growth at a moderate temperature ∼430 °C to form high-quality smooth ZnO layers for device structures. It was possible to reduce the growth temperature to 250–290 °C and obtain a smooth epitaxial template layer on sapphire (0 0 0 1) substrates with surface roughness less than 1 nm. After the high-temperature growth, the film surface undulations (roughness) increased to about 2 nm, but it is still quite smooth. The calculation of *c* and *a* lattice parameters by high-resolution x-ray diffraction shows that the *a* lattice parameter is fully relaxed at the growth temperatures but the *c* lattice parameter is dependent on the defect concentration in the growing film. A decoupling between *a* and *c* lattice parameters of the films is observed, which leads to abnormal Poisson's ratios ranging from 0.08 to 0.54. The decoupling of the lattice parameters is analysed based on growth characteristics and the presence of strain and defects in the grown films. We present our detailed studies on the nature of epitaxy, defects and interfaces by using comprehensive x-ray diffraction and high-resolution TEM studies.

(Some figures in this article are in colour only in the electronic version)

1. Introduction

Research on ZnO is in the forefront these days owing to its direct wide bandgap $E_g \sim 3.37$ eV and high excitonic binding energy ∼60 meV at room temperature (RT) [1] which makes it an attractive material for short wavelength optoelectronic device applications [2, 3]. In addition, ZnO can be alloyed with MgO and CdO to increase (blue shift) and decrease (red shift) the band gap, respectively, thus covering the entire range of visible spectrum [4–6]. The growth of device-quality ZnO thin films on substrates such as sapphire (0 0 0 1) involves a planar misfit exceeding 15%. Narayan and Larson [7] have shown that such a large planar misfit can be accommodated by the paradigm of domain matching epitaxy (DME), where integral multiples of lattice planes match across the film–substrate interface. In the specific case of ZnO/α-Al_2O_3 (0 0 0 1) sapphire, 6/7 and 5/6 domains were found to alternate to accommodate the misfit strain of 15.44%. Since the critical thickness under such a large misfit is less than one monolayer, the film can be relaxed from the beginning, as has been confirmed by *in situ* synchrotron studies [7]. The subsequent ZnO layers can be grown strain free, except for the differential thermal strain which is inherent to the growth temperature and the microstructural (defect) strain which

[4] Author to whom any correspondence should be addressed.

 © 2009 IOP Publishing Ltd Printed in the UK

depends on the growth ambient to some extent. Under this scenario, if the initial layer can be grown two-dimensional then the misfit dislocations can run across the film–substrate interface, generating very few threading dislocations. Thus, high-quality thin film heterostructures (having large misfit) can be grown by a two-step process in which initial layer is grown at a low temperature (LT) via two-dimensional growth. The thin film is fully relaxed except for residual thermal and defect strains. The initial layer can thus be used as a template to grow high-quality thin films at moderate temperatures, with fewer trapped defects and threading dislocations.

In this paper, we focus on structural and microstructural characteristics of thin films and show that the initial layer of ZnO on (0 0 0 1) sapphire can be grown epitaxially by pulsed laser deposition (PLD) via two-dimensional growth in the temperature range 230–290 °C. Subsequent growth in the temperature range 400–430 °C produces high-quality device layers with fewer defects and negligible residual strains. Improvement in the film quality by a two-step growth process has been demonstrated earlier for the III–V systems. Previous studies on ZnO [8–13] focused on high-temperature growth and films characterized by θ–2θ scans (which probe relaxation only along the c-axis) showed high quality (low FWHM values). It should be noted that θ–2θ scans provide information on alignment only along the c-axis (textured growth, one-axis alignment) and not in-plane alignment, which determines epitaxial growth (three-axis alignment). However, high-temperature growth leads to 3D growth with misaligned islands leading to the formation of small-angle grain boundaries (high FWHM values in ϕ scans). There have been recent reports on the growth of ZnO thin films on α-Al_2O_3 by employing a homo-buffer at LTs [14, 15]. However in these reports the LT buffers and the films were annealed at HT to improve the film quality. In contrast, in our study the films grown are thinner and only *in situ* annealing of the buffer for ramp-up to the film growth at a higher temperature was done. The FWHM of the (0 0 0 2) peaks and the strain in the film is less than that reported by Zheng *et al* [14]. It is pertinent to mention that in thin film heteroepitaxy the FWHM and the strain in the films decrease with increasing film thickness. In this paper, we report on initial stages of thin film growth and on the microstructural properties of ZnO thin films deposited on α-Al_2O_3(0 0 0 1) by a two-step growth process. In our study, we deposited a thin buffer ∼25 nm at two different LTs ∼250 and 290 °C. The epilayer ∼45 nm was deposited at ∼430 °C. Our study demonstrates that the buffer layer grown at LT grows epitaxially aligned with sapphire, is single crystal and shows a 2D growth mode. The 2D growth mode of the nucleation layer (NL) causes the misfit dislocations to run across the film–substrate interface and thus generates very few threading dislocations in the film. The growth of epitaxial ZnO films with a smooth surface at low growth temperatures presented in this paper opens exciting opportunities for the application of ZnO as a device template layer and transparent contact layers in LEDs and display devices.

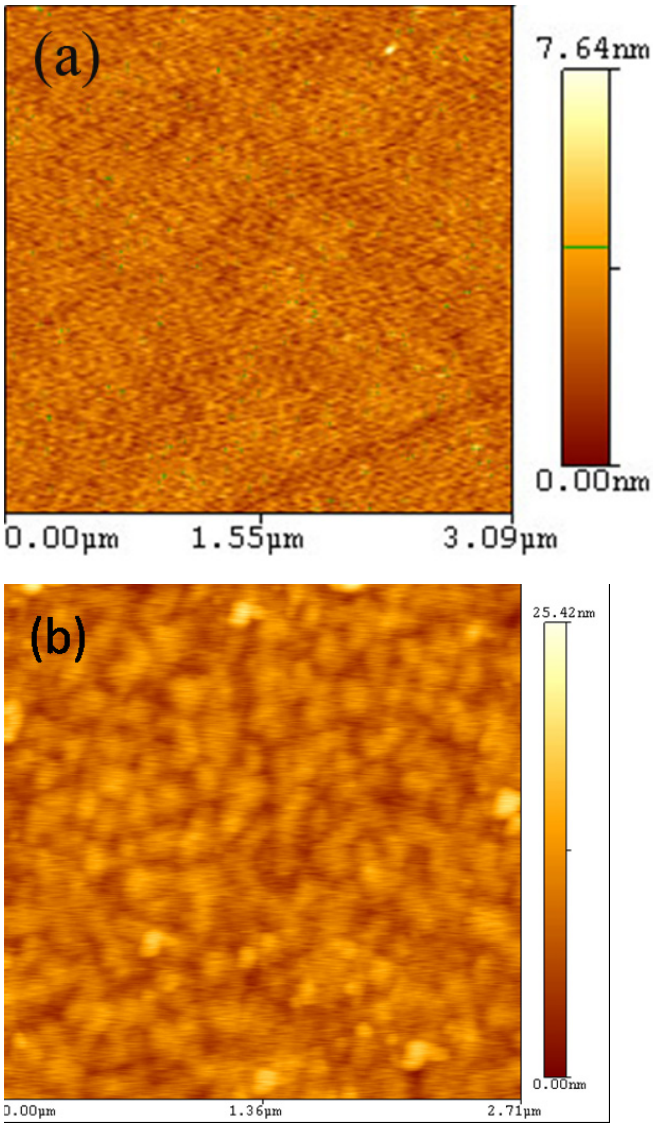

Figure 1. AFM images of the ZnO films deposited (*a*) at 250 °C showing a smooth surface (*b*) at 250 + 430 °C showing a 3D growth.

2. Experimental

ZnO thin films were grown on α-Al_2O_3 (0 0 0 1) substrate by ablating a polycrystalline ZnO target. The target was prepared by pressing and sintering high purity (99.9995%) ZnO powder at 800 °C for 8 h. A KrF excimer laser with a wavelength of 248 nm, pulse width of 25 ns and a fluence of 2–3 J cm^{-2} was used. The base vacuum prior to deposition was 10^{-7} Torr and films were deposited at an O_2 partial pressure of 10^{-5} Torr. The LT deposition of ∼25 nm thick buffer was done at two temperatures ∼250 and 290 °C. Thick films ∼45 nm were deposited on the buffer layers to study the effect of the buffer on the epitaxy of ZnO films. Low-resolution (high-intensity) x-ray diffraction scans with a slit after the samples were used to determine the lattice structure and the epitaxial orientations of the film with respect to the substrate. Subsequent high-resolution x-ray scans used a Ge analyzer crystal after the sample to quantitatively determine the lattice parameters and the correlation lengths. Structural characterization was done

Table 1.

	250 °C	290 °C	250 + 430 °C	290 + 430 °C
a (Å) $3.252A(RT)^2$	3.246	3.245	3.242	3.243
c(Å) $5.213A(RT)^2$	5.233	5.224	5.216	5.215
FWHM $\Delta 2\theta(0\,0\,0\,2)$ °	0.676	0.662	0.180	0.172
L (nm) (correlation length (0 0 0 2))	12.84	13.12	48.25	50.49
FWHM $\Delta 2\theta(1\,0\,-1\,1)$°	0.650	0.580	0.250	0.246
L (nm) (correlation length (1 0 −1 1))	13.43	15.05	34.84	35.41
Strain along c direction% (measured)	0.393	0.218	0.056	0.045
Strain in-plane% (measured)	−0.17	−0.19	−0.28	−0.26
Thermal strain% (calculated)	−0.10	−0.12	−0.18	−0.18
Poisson's ratio	0.54	0.37	0.09	0.08

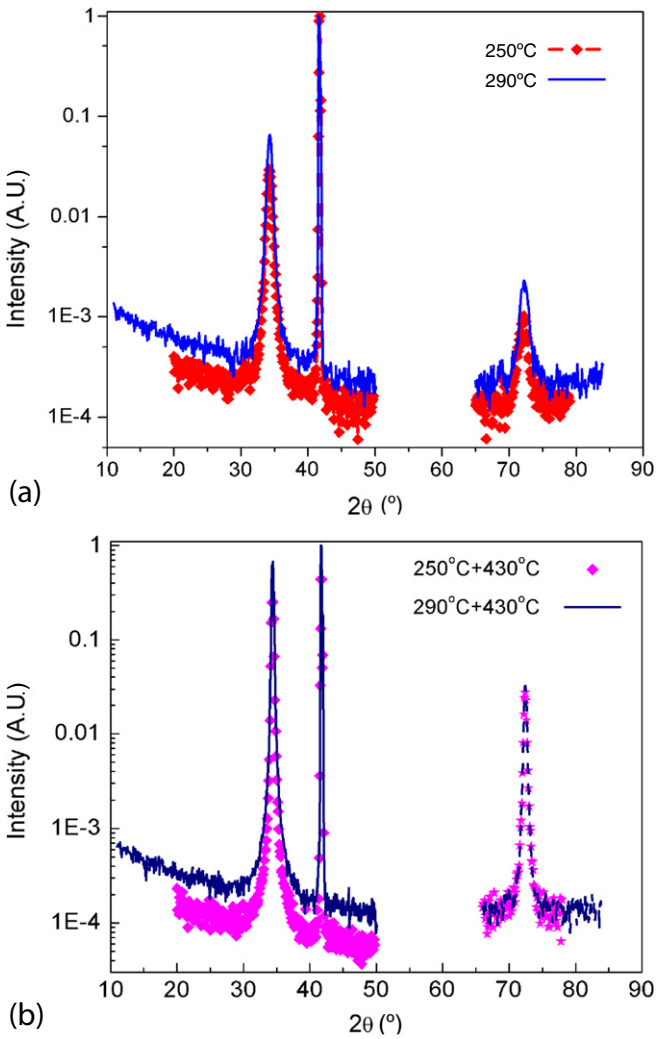

Figure 2. Low-resolution θ–2θ scans (a) for the buffer layers grown at 250 °C and 290 °C and (b) for epilayer grown at ∼430 °C on the buffer layers.

using a JEOL 2010F electron microscope operating at 200 kV with a point-to-point resolution of 1.8 Å and STEM-Z of 1.2 Å with a Gatan image filter (GIF) attachment. The samples for TEM were prepared using our conventional sample preparation techniques which included mechanical polishing, dimpling and Ar^+ ion milling. The surface morphology was studied by atomic force microscopy (AFM) in the ac mode.

3. Results and discussions

The surface morphology of the ZnO films grown at LTs (250 and 290 °C) and at ∼430 °C was studied by AFM. Figures 1(a) and (b) show the AFM images for the LT buffer grown at 250 °C and for the epilayer grown at 430 °C on the LT buffer, respectively. The surface morphology of the buffer layer shows a very smooth surface with a measured surface roughness of less than 1 nm. The growth mode is envisaged to be two-dimensional. The surface morphology of the epilayer grown on the LT buffer shows a surface roughness of about 2 nm. The presence of strain is known to cause surface undulations in the films [16] and it is consistent with the increase in the surface roughness of the film grown at higher temperatures. We propose that the increase in the surface roughness is due to the remnant thermal strain which characteristically increases with growth temperature and also due to the microstructural strain which depends partly upon the growth ambient. This increase in roughness is consistent with x-ray diffraction results on in-plane strain measurements (table 1).

Figures 2(a) and (b) show low-resolution θ–2θ scans for the grown buffer layers and for subsequent growth of the film at ∼430 °C on the buffer layers. These scans show the presence of only (0 0 0 2) and (0 0 0 4) peaks of ZnO and the (0 0 0 6) peak from the Al_2O_3 (0 0 0 1) substrate indicating c-axis aligned growth of ZnO at LTs and also in the subsequent deposition of the film at ∼430 °C. Figures 3(a) and (b) show the ZnO(0 0 0 2) rocking curves measured through the ZnO(0 0 0 2) peak at different ϕ (0°, 180°) positions for the buffer grown at 250 °C and the epilayer grown at 430 °C on the buffer layer. Figures 3(c) and (d) show the θ scans through ZnO(0 0 0 2) peaks at different ϕ (0°, 180°, 90°, −90°) positions for the buffer grown at 290 °C and the epilayer grown at 430 °C on the buffer. The superposition of the scans at different azimuthal positions in the buffer layers as well as in the epilayer growth indicates that the ZnO(0 0 0 2) planes are well aligned and parallel to the Al_2O_3(0 0 0 6) planes. It is observed that the mosaic spread ($\Delta\theta$) of the (0 0 0 2) planes of the films grown at 290 °C is less than that of the films grown at 250 °C. This observation is also reflected in the mosaic spread of the films grown at 430 °C on the buffer layers i.e. $\Delta\theta_{\mathrm{Film}(250\,^\circ\mathrm{C}+430\,^\circ\mathrm{C})} > \Delta\theta_{\mathrm{Film}(290\,^\circ\mathrm{C}+430\,^\circ\mathrm{C})}$. From these observations we can infer that the buffer grown at LT influences subsequent film growth. Bragg's law was used to

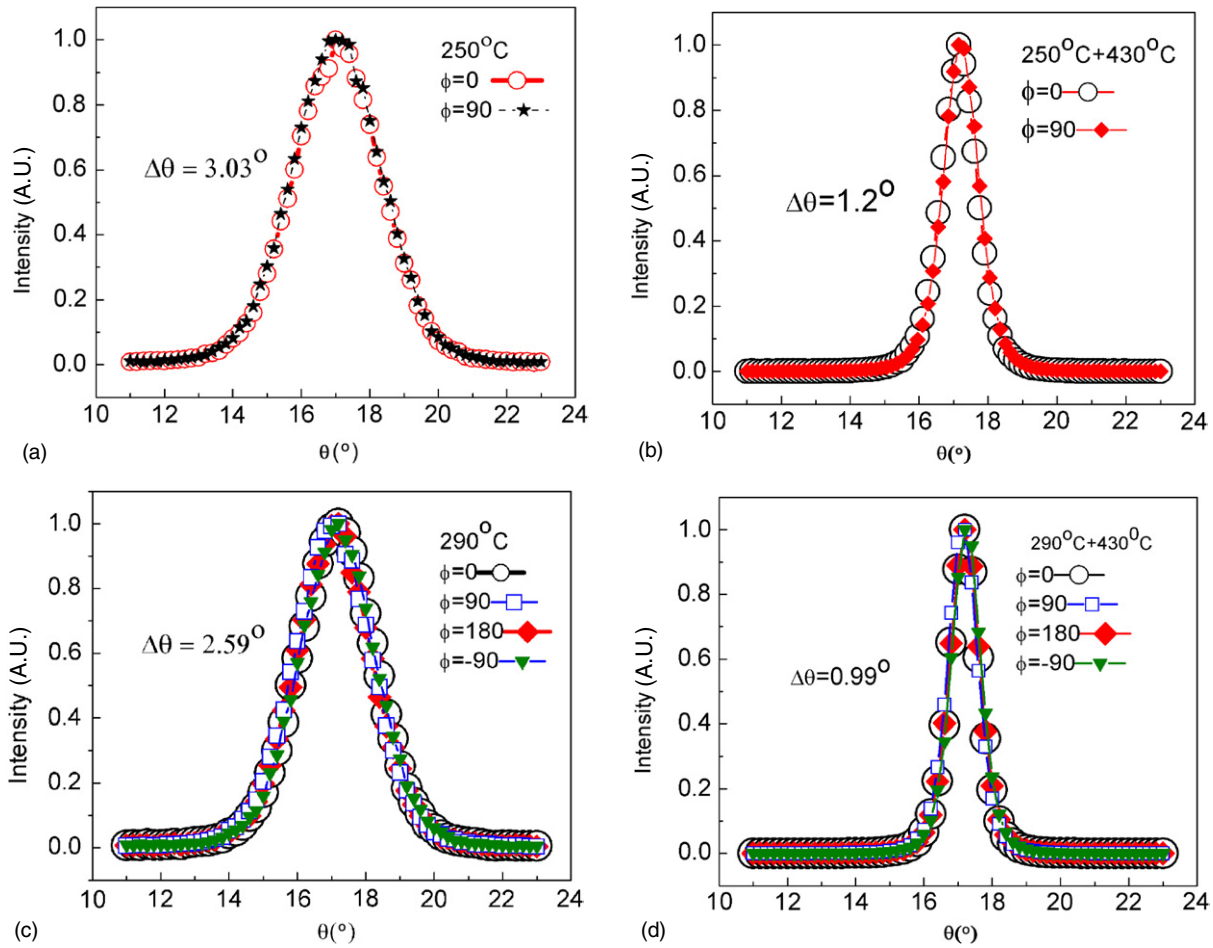

Figure 3. Rocking curves measured through the ZnO(0 0 0 2) peak for (*a*) the buffer grown at 250 °C, (*b*) the epilayer grown at 430 °C on the buffer, (*c*) the buffer grown at 290 °C and (*d*) the epilayer grown at 430 °C on the buffer.

determine the *a* and *c* lattice parameters from high-resolution θ–2θ scans through ZnO(0 0 0 2) and (1 0 −1 1) peaks (not shown) and are listed in table 1. The values of the *a* lattice constant indicate the presence of a compressive strain in both the buffer and the epilayer grown on the buffer. The strain in thin films has three contributing terms: lattice strain, thermal strain and microstructural strain. The out-of-plane and in-plane lattice strains in the film were determined by using the expression: $\varepsilon = (l_f - l_b)/l_b$, where l_f is the measured lattice parameter of the film and l_b is the bulk value of the corresponding lattice parameter. The thermal component of the film strain was calculated by using the expression $\varepsilon_{thermal} = (\alpha_{sub} - \alpha_{film})\Delta T$ where $\alpha_{sub}(\alpha_{sap} = 7.5 \times 10^{-6}\,K^{-1})$ [2] and $\alpha_{film}(\alpha_{ZnO} = 2.9 \times 10^{-6}\,K^{-1})$ [2] are the coefficients of thermal expansion of the film and the substrate, ΔT is the difference in temperature between the growth temperature and the RT. The microstructural strain is associated with trapped point defects (like Zn interstitials and oxygen vacancies) and extended defects (dislocations, stacking faults (SFs) and twins), which are to some extent dependent on the growth ambient. From our calculations in table 1 we find that whereas ε_{zz} becomes almost negligible for the epilayers grown on the buffer layers, the value of ε_{xx} for the epilayers grown on the buffer layers is greater than the value of ε_{xx} for the LT buffer layers. The measured values of the *c* and *a* lattice parameters show that the observed relaxation in them is not in concert with each other leading to a variation in Poisson's ratio (ν) from 0.08 to 0.54 as shown by the calculated values of ν in table 1 compared to a normal value of $\nu = 0.35$ for ZnO [2]. The value of ν was calculated by using the expression $\varepsilon_{zz} = (-2\nu/1 - \nu)\varepsilon_{xx}$, where ε_{zz} is the measured strain along the *c*-axis and ε_{xx} is the measured strain along the *a*-axis. The anomaly in the behaviour of lattice parameters can be explained by the controlled kinetics of the growth process and the difficulty of dislocation nucleation. We propose that during initial stages of film growth the in-plane strain is fully relaxed within the critical thickness of less than one monolayer by the paradigm of DME where integral multiples of planes match across the film–substrate interface [7]. The increase in the in-plane strain with growth temperature is explained by the thermal strain in the film which is inherent to the growth temperature of the film and the differences in the coefficient of thermal expansion of the film and the substrate. No further in-plane relaxation is allowed after initial stages of growth because of the barrier to dislocation nucleation and propagation. Also the critical resolved shear stress needed to generate dislocations by plastic deformation in *a*- and *c*-planes (normal and parallel) is zero. The critical resolved shear stress (τ_r) is given by $\tau_r = \sigma(\cos\phi)(\cos\lambda)$, where $\sigma = \sigma_{xx} = \sigma_{yy}$ is the stress in the film plane, ϕ is the angle between the plane normal and σ, and λ

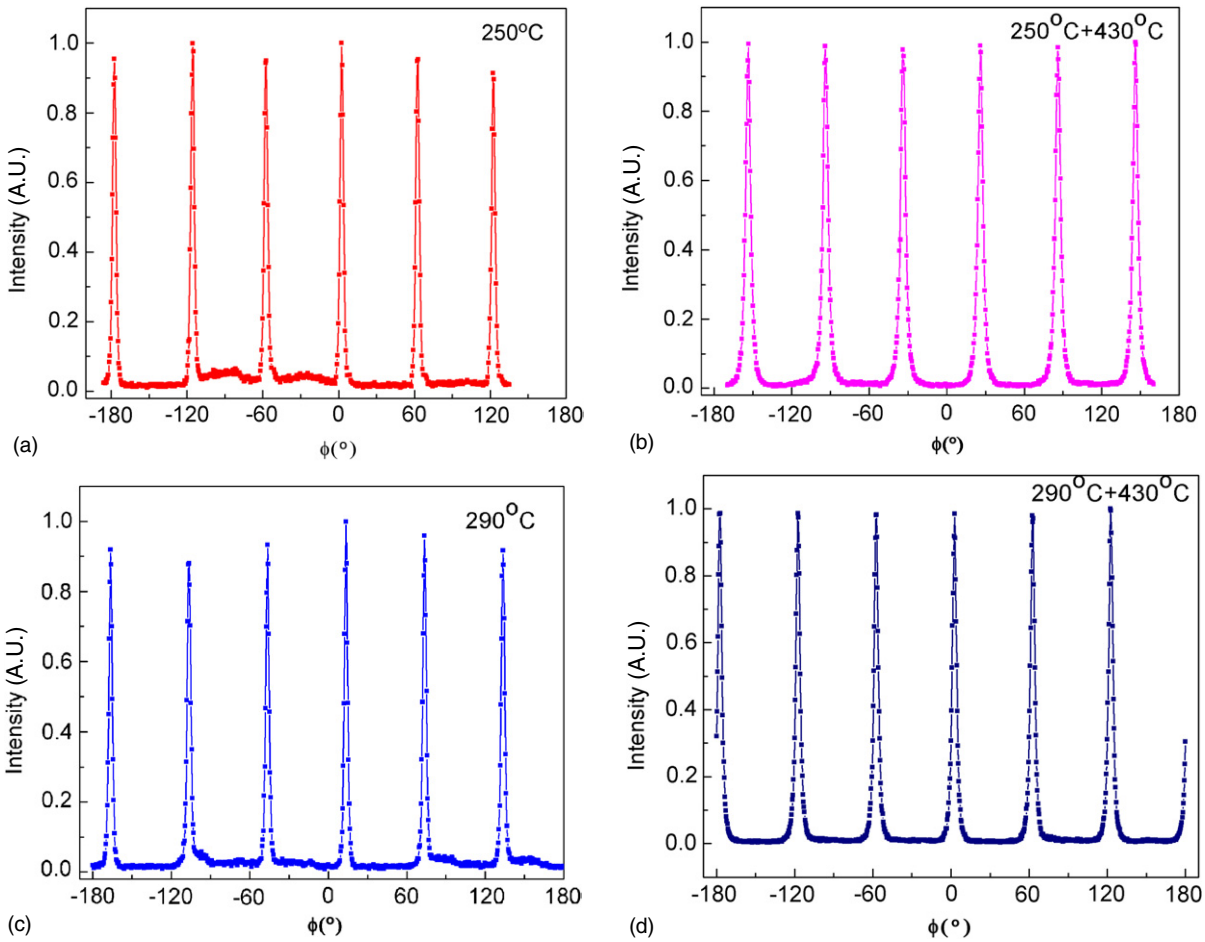

Figure 4. ϕ-scans through ZnO(1 0 −1 1) planes of the samples clearly show the six-fold symmetry of the ZnO films in all the samples.

is the angle between the slip direction and σ. As the film growth proceeds, point defects and planar defects (such as twins and SFs) are trapped in the deposited film. The presence of native point defects in ZnO is known to cause local lattice relaxation due to stretching of the Zn–O bond surrounding the defect [17]. The global relaxation observed in the c lattice parameter at LT growth of the buffer is explained by the presence of native point defects which get incorporated during growth of the buffer layers, because of low migration energies of oxygen vacancies and Zn interstitials. Following the theoretical calculations and results of Janotti and Van de Walle [17] it is proposed that the point defects introduced during LT growth of the buffer get annealed out during temperature ramp-up for the growth of ZnO epilayer. The annealing out of defects during the temperature ramp-up explains the convergence of the c lattice parameter towards the unstrained value for the epilayers grown on the buffer layers. The increase in c requires point defects causing outward expansion [17], which can result from zinc interstitials, charged oxygen vacancies and SFs Our study thus shows that it is possible to grow completely lattice relaxed thin films <75 nm thick at temperatures as low as 450 °C. We find that, whereas lattice strain in the film is relaxed, the thermal strain is not easily relaxed because of inherent difficulty in nucleation and propagation of dislocations along with geometrical constraints for resolved shear stress to generate dislocations. This strain is expected to play an important role in affecting the device properties of thin films, for example, the piezoelectric effects with strain affect electronic transition processes.

The Scherrer equation was used to estimate the correlation length from the x-ray peak width and is listed in table 1. For a perfect film the correlation length should be approximately equal to the film thickness. The presence of defects, however, reduces the correlation length because the lattice planes are not separated by the correct d-spacing and hence lose coherence. The calculated values of the correlation length indicate that the buffer deposited at 290 °C is slightly more coherent than the buffer grown at 250 °C. For the film deposited at 430 °C on these buffers the out-of-plane coherence is better than the in-plane coherence. For a perfect ZnO thin film on (0 0 0 1)Al_2O_3, the measured correlation length should be the smallest for the planes parallel to the surface i.e. for (0 0 0 1) ZnO c-planes because the film is the thinnest in this direction and the in-plane correlation length measured using ZnO (1 0 −1 1) should be very large (width of the sample ∼mm) and a measurement would be limited by the instrumental resolution. For a perfect c-axis wurtzite ZnO thin film, the correlation length for the ZnO(1 0 −1 1) planes should be about twice as large as for the (0 0 0 1) because the film is effectively twice as thick in this direction, i.e. more planes are scattering coherently to make a sharper peak. The fact that the measured (1 0 −1 1) correlation length is actually comparable to or smaller than the

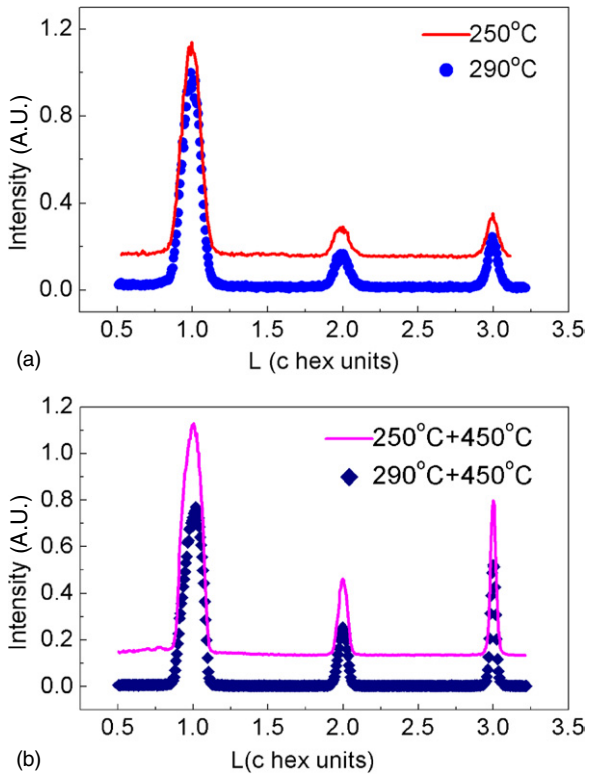

Figure 5. *L*-scans through ZnO(1 0 −1 L) for all four samples show peaks at integral positions indicating a hexagonal ABAB... stacking in the samples.

out-of-plane correlation length suggests the presence of defects which are difficult to anneal and cause a faster degradation of the perfection in the in-plane direction. To establish epitaxial growth (three-axis alignment) ϕ-scans through ZnO(1 0 −1 1) planes of the samples were measured. The ϕ-scans in figures 4(*a*)–(*d*) show the six-fold symmetry of the ZnO film in all the samples. There is a 30° rotation between the in-plane ZnO and Al_2O_3 directions giving an in-plane orientation relationship ZnO[1 1 −2 0]//Al_2O_3[1 0 −1 0]. Shan *et al* [18] have reported the absence of the reflection peaks showing six-fold symmetry in the ϕ-scans at temperatures less than 300 °C and have mentioned that epitaxial growth can be achieved at temperatures 400 °C and above only. On the other hand, the ϕ-scans in our studies show that films deposited at LTs also grow epitaxially aligned with sapphire substrate and show the presence of only the commonly aligned domains. Additional information about the microstructure of the film was revealed by *L*-scans which give information about the stacking sequence of the ZnO planes parallel to the surface. The *L*-scans through ZnO(1 0 −1 *L*) for all four samples in figures 5(*a*) and (*b*) show peaks at integral positions, which is consistent with hexagonal wurtzite ABAB... stacking in all the samples.

Transmission electron microscopy was used to investigate the details of DME, the interface structure and the nature of defects in the ZnO/α-Al_2O_3 heterostructure. Figures 6(*a*) and (*b*) show the low-magnification TEM images of the interface from samples 1 and 3. From the images we see that the buffer layer has a thickness of ∼25 nm and the epilayer grown at HT on the buffer has a thickness of ∼45 nm. Figures 6(*c*) and (*d*) show the selected area electron diffraction (SAED) pattern from the interface regions of samples 1 and 3. The SAED patterns were taken along the [0 −1 1 0] sapphire zone axis and give the following epitaxial relationship between the film and the substrate: (0 0 0 2)ZnO//(0 0 0 6)α-Al_2O3; [2 −1 −1 0]ZnO//[0 −1 1 0]α-Al_2O_3. This relationship corresponds to a 30° in-plane rotation of the film with respect to the substrate and an alignment of (0 1 −1 0) (spacing of 2.814 Å) planes of ZnO with (−2 1 1 0) (spacing of 2.379 Å) planes of α-Al_2O_3. The epitaxial growth of ZnO on α-Al_2O_3 is controlled by DME [7] where integral multiples of lattice planes match across the interface. Under these conditions seven planes of sapphire match with six planes of ZnO across the interface as can be seen in the FFT images shown in figures 6(*g*) and (*h*). Figures 6(*e*) and (*f*) are HRTEM images from the interface regions of samples 1 and 3. These images show an atomically sharp interface between ZnO and α-Al_2O_3 even at LT. Compared to other film growth techniques, in PLD the growth of 2D single crystal films is enabled at temperatures as low as 250–300 °C by the energetics of the PLD process. In PLD the kinetic energies of the ablated species lie in a range that promotes surface mobility of the adatoms at the surface to enable their migration to thermodynamically stable sites and thereby promote epitaxial and 2D growth of the films even at a low temperature. The images indicate the presence of planar defects namely SFs in the region close to the interface. Compared to the GaN NL which shows a crystal structure containing both the cubic and the wurtzitic phase of GaN which is attributed to the ordered nature of SFs in GaN [19], the SFs in the ZnO buffer are proposed to be random in nature. The random nature of the faults in the ZnO buffer is also confirmed by the x-ray *L*-scans which show only a hexagonal signature.

In conclusion, we have grown single crystal epitaxial thin films of ZnO at LTs on sapphire by PLD using a two-step process. Detailed microstructural characterization of the thin films by x-ray diffraction and HRTEM confirms the epitaxial growth of the film even at low temperatures. The decoupling observed between the *c* and *a* lattice parameters leads to abnormal Poisson's ratio varying from 0.08 to 0.54. We have shown that within the limits of thermal strain, the in-plane strain is fully relaxed at the growth temperature by the paradigm of DME. The relaxation of the *c*-axis is controlled by the defects trapped during the growth process. Since dislocations are not nucleated presumably due to high nucleation and migration barriers and zero resolved shear stress in normal planes, no relaxation is allowed in the *a*-axis. Thus, the *a*-axis remains the same and the *c*-axis relaxes depending upon the concentration of point defects and SFs and their annealing during growth. Our study shows that even though it is possible to grow completely relaxed films at temperatures less than 500 °C, small amounts of residual thermal strain less than a few-tenths of a per cent remains. AFM measurements show that the grown films have very small values of surface roughness. The low-temperature buffer has a very smooth surface, grows two dimensionally and is found to influence the subsequent growth of the epi-ZnO film. The 2D template and the high-quality epitaxial growth of films at lower temperatures presented in this study can be used to grow smooth and

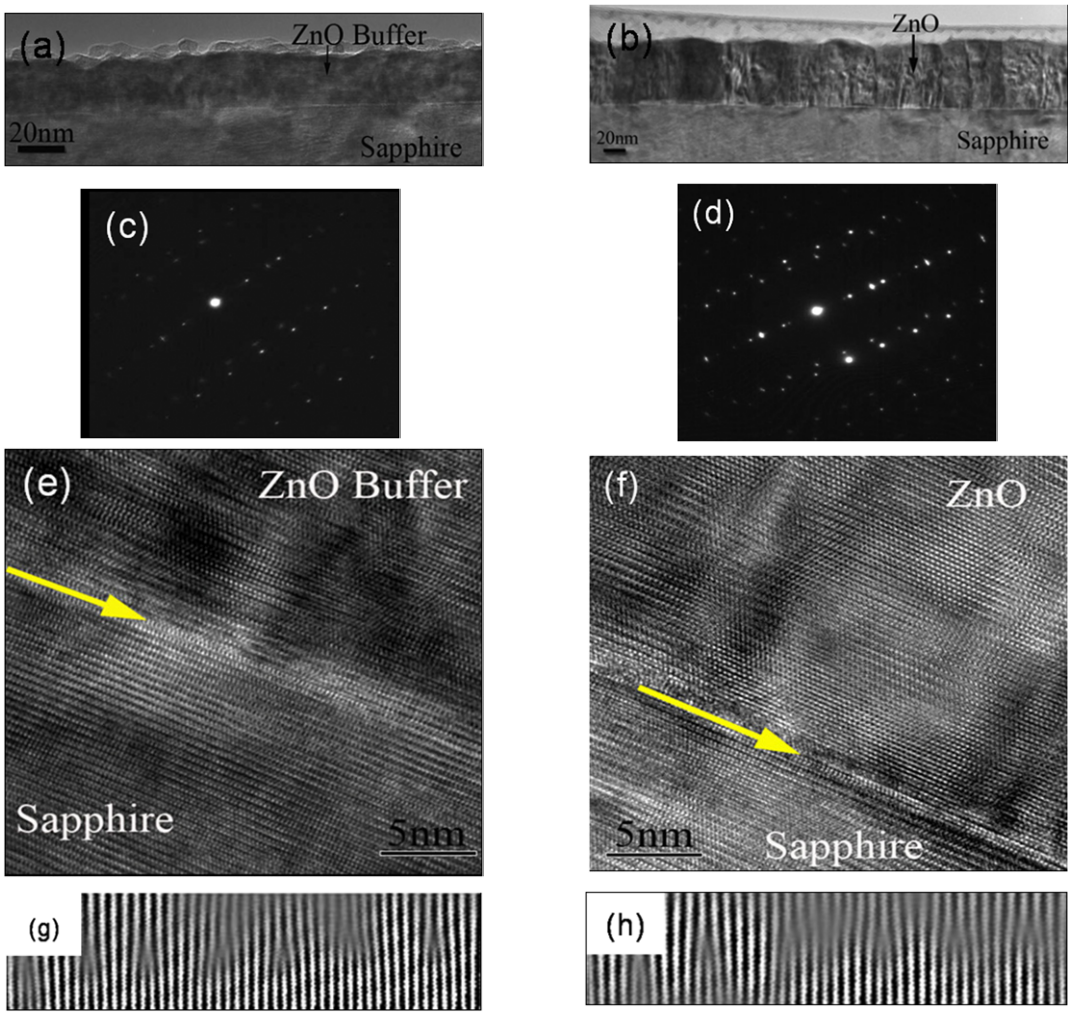

Figure 6. Low-magnification TEM images of the interface from (*a*) sample 1 and (*b*) sample 3. Selected area diffraction (SAD) pattern from the interface regions taken along the [−2 1 1 0] sapphire zone axis for (*c*) sample 1 and (*d*) sample 3. HRTEM images from the interface regions of (*e*) sample 1 and (*f*) sample 3. Corresponding FFT image of the interface demonstrating matching of integral multiples of lattice planes across the ZnO/sapphire interface: (*g*) sample 1 and (*h*) sample 3.

less defective films for contact layers and in integration of devices on substrates like plastics where HT processing poses a limitation. These results of epitaxial growth of single crystal ZnO films at LTs will be supplemented with our further work on the electrical and optical properties of the films to provide further insight into the effect of buffer and thermal strain on the quality of the film and the nature of residual defects in the film.

Acknowledgments

This research was supported by the National Science Foundation. The work was also supported by the DOE Office of Science, DMS under contract with ORNL, managed by UT-Battelle, LLC.

References

[1] Bagnall D M, Chen Y F, Zhu Z, Yao T, Koyama S, Shen M Y and Goto T 1997 *Appl. Phys. Lett.* **70** 2230

[2] Özgür Ü, Alivov Ya I, Liu C, Teke A, Reshchikov M A, Doğan S, Avrutin V, Cho S J and Morkoç H 2005 *J. Appl. Phys.* **98** 041301

[3] Pearton J, Norton D P, Ip K, Heo Y W and Steiner T 2003 *Superlatt. Microstruct.* **34** 3

[4] Narayan J, Sharma A K, Kvit A, Jin C, Muth J F and Holland O W 2002 *Solid State Commn.* **121** 9

[5] Narayan J 2002 *US Patent* No 6423983 (23 July)

[6] Narayan J 2003 *US Patent* No 6518 077 (11 February)

[7] Narayan J and Larson B C 2003 *J. Appl. Phys.* **93** 278

[8] Wang X, Yang S, Wang J, Li M, Jiang X, Du G, Liu X and Chang R P H 2002 *Opt. Quantum Electron.* **34** 883

[9] Kobayashi K, Matsubara T, Matsushima S, Shirakata S, Isomura S and Okada G 1995 *Thin Solid Films* **266** 106

[10] Johnson L M A, Fujita S, Rowland W H Jr, Hughes W C, Cook J W Jr and Schetzina J F 1996 *J. Electron. Mater.* **25** 855

[11] Chen Y, Bagnall D M, Zhu Z, Sekiuchi T, Ki-tae Park, Hiraga K, Yao T, Koyama S, Shen M Y 1997 *J. Cryst. Growth* **181** 165

[12] Sankur H and Cheung J T 1983 *J. Vac. Sci. Technol.* A **1** 1806

[13] Narayan J, Dovidenko K, Sharma A K and Oktyabrsky S 1998 *J. Appl. Phys.* **84** 2597

[14] Zheng W, Liao Y, Li L, Yu Q, Wang G, Li Y and Fu Z 2006 *Appl. Surf. Sci.* **253** 2765
[15] Jung Y-S, Kononenko O, Kim J-S and Choi W-K 2005 *J. Cryst. Growth* **274** 418
[16] Lorenz K, Gonsalves M, Kim W, Narayanan V and Mahajan S 2000 *Appl. Phys. Lett.* **77** 3391
[17] Janotti A and Van de Walle C G 2007 *Phys. Rev.* B **76** 165202
[18] Shan F K, Liu G X, Lee W J and Shin B C 2007 *J. Appl. Phys.* **101** 053106
[19] Narayan J, Pant P, Chugh A, Choi H and Fan J C C 2006 *J. Appl. Phys.* **99** 054313